

# HILIGT, Upper Limit Servers I - Overview<sup>\*</sup>

Saxton, R.D.<sup>a</sup>, König, O.<sup>b</sup>, Descalzo, M.<sup>c</sup>, Belanger, G.<sup>d</sup>, Kretschmar, P.<sup>d</sup>, Gabriel, C.<sup>d,e</sup>, Evans, P.A.<sup>f</sup>, Ibarra, A.<sup>g</sup>, Colomo, E.<sup>a</sup>, Sarmiento, M.<sup>h</sup>, Salgado, J.<sup>g</sup>, Agrafajo, A.<sup>g</sup>, Kuulkers, E.<sup>i</sup>

<sup>a</sup>*Telespazio U.K. Ltd. for the European Space Agency (ESA), European Space Astronomy Centre (ESAC), Camino Bajo del Castillo s/n, 28692 Villanueva de la Cañada, Madrid, Spain*

<sup>b</sup>*Dr. Karl-Remeis-Sternwarte and Erlangen Centre for Astroparticle Physics, Friedrich-Alexander-Universität Erlangen-Nürnberg, Sternwartstr. 7, 96049 Bamberg, Germany*

<sup>c</sup>*Department of Electrical Engineering, Technical University of Denmark (DTU), Ørstedts Plads 326, 2800 Kongens Lyngby, Denmark*

<sup>d</sup>*European Space Agency (ESA), European Space Astronomy Centre (ESAC), Camino Bajo del Castillo s/n, 28692 Villanueva de la Cañada, Madrid, Spain*

<sup>e</sup>*Committee on Space Research (COSPAR) – 2, place Maurice Quentin, 75039 Paris Cedex 01, France*

<sup>f</sup>*University of Leicester, X-ray and Observational Astronomy Group, School of Physics and Astronomy, University Road, Leicester, LE17RH, UK*

<sup>g</sup>*QUASAR Science Resources for the European Space Agency (ESA), European Space Astronomy Centre (ESAC), Camino Bajo del Castillo s/n, 28692 Villanueva de la Cañada, Madrid, Spain*

<sup>h</sup>*Aurora Technology B.V for the European Space Agency (ESA), European Space Astronomy Centre (ESAC), Camino Bajo del Castillo s/n, 28692 Villanueva de la Cañada, Madrid, Spain*

<sup>i</sup>*European Space Agency (ESA), European Space Research and Technology Centre (ESTEC), Keplerlaan 1, 2201 AZ Noordwijk, The Netherlands*

---

## Abstract

The advent of all-sky facilities, such as the Neil Gehrels Swift observatory, the All Sky Automated Search for Supernovae (ASAS-SN), *eROSITA* and *Gaia* has led to a new appreciation of the importance of transient sources in solving outstanding astrophysical questions. Identification and catalogue cross-matching of transients has been eased over the last two decades by the Virtual Observatory but we still lack a client capable of providing a seamless, self-consistent, analysis of all observations made of a particular object by current and historical facilities. HILIGT is a web-based interface which polls individual servers written for *XMM-Newton*, *INTEGRAL* and other missions, to find the fluxes, or upper limits, from all observations made of a given target. These measurements are displayed as a table or a time series plot, which may be downloaded in a variety of formats. HILIGT currently works with data from X-ray and Gamma-ray observatories.

**Keywords:** Catalogs, Surveys, X-rays: general, Instrumentation: detectors, Upper limit, Aperture photometry

---

## 1. Introduction

Since the first discovery of X-ray emission from SCO X-1 in 1962 by the Aerobee 150 sounding rocket (Giacconi et al., 1962), X-ray telescopes have been flown on satellites on a regular basis. Their observations provide a record of the flux emitted from the brightest sources which now stretches back for 50 years. Detected sources from the majority of these missions are provided in specific catalogues (e.g. Evans et al., 2010; Webb et al., 2020; Evans et al., 2020) or are served by the comprehensive multi-mission archive hosted at HEASARC (Heasarc Team, 1995)<sup>1</sup>. Many missions have also left a legacy of sky images. These allow upper limits to fluxes to be found from sky positions where a source has not been detected and catalogued.

As new sources are detected, due to the introduction of more sensitive instruments or because they have transitioned into a brighter state, it is of interest to know how previous observations of that position on the sky can constrain the history of the flux. For known sources, while targeted observations are often

covered by catalogues, serendipitous non-detections and detections of lower flux may not be. To fully exploit the datasets of all X-ray missions, functionality is needed capable of returning catalogue values or of calculating upper limits from images. In this way, historical light curves can be generated using the full dataset of each mission.

To this end a suite of flux / upper-limit servers have been written, one for each mission, which run in parallel and either forward on results from the best available on-line catalogue or analyse the images and return upper limits from a given position (Fig. 1).

In this paper we review the design and describe the input parameters and the fields returned by each server. A companion paper (König et al. 2021; hereafter Paper II) describes in detail how each individual server has been constructed. A brief summary of the missions which are currently supported is given in Table 1. Results are returned as a Representational State Transfer (REST) service which may be called by any suitable client; a web client with plotting facilities has been produced and is described in detail in Sect. 2.3. The collection of servers and the web client together are called the High-energy Light curve GeneraTor (HILIGT) which replaces an earlier upper limit server hosted at the *XMM-Newton* science operations

---

<sup>\*</sup><http://xmmuls.esac.esa.int/hiligt>

Email address: richard.saxton@sciops.esa.int (Saxton, R.D.)

<sup>1</sup><https://heasarc.gsfc.nasa.gov/>

centre (SOC) that worked exclusively with *XMM-Newton* data<sup>2</sup>.

## 2. Mission count rate and flux servers

The fundamental property measured by a photon counting detector is the background-subtracted count rate. This can be converted into an energy flux by convolving with the efficiency and spectral resolution of the detector as a function of energy and by assuming a spectral model.

Each HILIGT server either returns the source count rate and error with the equivalent flux derived from the input spectral model, or calculates the upper limit on the source count rate, at a user-selectable 1,2 or 3- $\sigma$  level, with the equivalent upper limit on the flux.

To enable fluxes to be compared between missions a standard set of energy bands have been defined: 0.2–2 keV (soft), 2–12 keV (hard) and 0.2–12 keV (total). The one current exception is *INTEGRAL* which uses the three bands 20–40, 40–60 and 60–100 keV. These ranges have been set as a compromise based on the actual energy bands of the mission instrumentation (see Table 1).

The processing flow of a server is given in Fig. 2 and consists of the following steps.

- Find all observations which contain a given set of equatorial coordinates (RA, Dec). Ultimately this is done by searching a database for image footprints which contain the sky position. The derivation of the footprints for each mission is described in Paper II and the comparison is made using the *pgsphere* package<sup>3</sup>, which is in some cases, for example for the *XMM-Newton* slew and pointed data, provided by a Table Access Protocol (TAP; Dowler et al., 2019) call.
- Get catalogue entries for this position. Catalogue fields, principally the source count rate and error, are accessed by making a TAP call<sup>4</sup> for *XMM-Newton* pointed data or by using the *w3Browse* facility provided at HEASARC<sup>5</sup>. Cross-matching with catalogues is carried out using a radius which takes into account the systematic positional error of the given catalogue and the likelihood of source confusion. Specific details are given in Paper II, Section 3.10.
- Calculate an upper limit for the sky position in images where a catalogue entry is not available, using aperture photometry.

This calculation relies on knowledge of the instrument vignetting and the Point Spread Function (PSF) which is

used to calculate the encircled energy function (EEF; the fraction of counts which lie within the extraction region). In order to provide a practical distinction between a detection and a non-detection, a decision has been taken to return a flux if the background-subtracted count rate is  $\geq 2$  times the error and otherwise return an upper limit at a user-selectable confidence level of 1, 2 or 3 sigma. The upper limit calculation uses Bayesian statistics based on the algorithm given in Kraft et al. (1991). We give a description of this calculation in Paper II.

- Calculate the flux from the count rate. This is done by multiplying by a factor, based on a provided spectral model. While in practise the spectral model of an astrophysical object can be very complicated, for simplicity in passing parameters, the model is currently limited to either a power-law with index,  $\Gamma = 0.5, 1.0, 1.5, 1.7, 2.0, 2.5, 3.0, 3.5$ , or a black-body of temperature  $kT = 60, 100, 300, 1000$  eV, attenuated by a neutral absorber of column,  $N_H = 1 \times 10^{20}, 3 \times 10^{20}, 1 \times 10^{21}$  cm<sup>-2</sup>. These values sample the typical observed spectra of sources and include the spectrum used to calculate fluxes in the *XMM-Newton* catalogue ( $\Gamma = 1.7, N_H = 3 \times 10^{20}$  cm<sup>-2</sup>, which is based on the average X-ray spectrum of an AGN (e.g. Turner and Pounds, 1989)). Conversion factors have been hard-coded into the server software for efficiency and were originally calculated using the PIMMS package (Mukai, 1993) or inferred from the relevant literature (Forman et al., 1978; Kaluzienski, 1977; Warwick et al., 1981; Wood et al., 1984; Nugent et al., 1983).

An alternative approach would be to pre-calculate and store fluxes for each catalogued source, for each spectral model, and make them available to HILIGT through a TAP server. While this would result in a performance improvement it would prove rather inflexible, as updates would be needed if the default spectral models were changed or if our understanding of the instrument calibration changed. It would also be unviable should the system be updated to allow the user to choose a spectral model on-the-fly.

### 2.1. Inter-mission cross-calibration

Significant community effort is put into the cross-calibration of X-ray detectors by the International Astronomical Consortium for High-Energy Calibration (IACHEC; Sembay et al., 2010). Recent missions, such as *XMM-Newton*, *Swift*, *NuSTAR*, *SUZAKU* and *Chandra* are found to return consistent fluxes to within 10–15% (Madsen et al., 2017a). For the older missions, the factors to convert count rate into flux tend to be based on observations of the Crab nebula (see Paper II), which has a power-law spectrum of  $\Gamma = 2.1$ . Fluxes are then only strictly valid for similar spectral shapes and furthermore the Crab flux and spectral shape are known to vary at the level of a few percent (Madsen et al., 2017b). To compensate for this, in the returned flux for these missions a systematic error of magnitude 30% (*Vela 5B*), 15% (*Ariel V*), 20% (*HEAO-1*) and 20% (*Uhuru*) is added in quadrature to the statistical error.

<sup>2</sup>A comprehensive upper limit server dedicated to the *XMM-Newton* EPIC cameras called FLIX is available at <https://www.ledas.ac.uk/flix/flix.html>

<sup>3</sup><https://pgsphere.github.io>

<sup>4</sup><http://nxs.a.esac.esa.int/tap-server/tap>

<sup>5</sup><https://heasarc.gsfc.nasa.gov/W3Browse/w3browse-help.html>

An alternative approach would have been to use the HEASARC TAP service.

Table 1: Currently supported missions

Mission	Instrument(s)	modes <sup>a</sup>	Data source <sup>b</sup>	Period (year)	Energy range <sup>c</sup> (keV)
VELA 5B	ASM	survey	CAT	1969-1979	3–12
Uhuru		survey	CAT	1970-1973	2–20
Ariel-V	ASM, SSI	survey	CAT	1974-1980	2–18
Heao-1	A1	pointed	CAT	1977-1979	0.25–25
Einstein	IPC, HRI	pointed	CAT, UL	1978-1981	0.15–4.0
EXOSAT	LE, ME	slew, pointed	CAT, UL	1983-1986	0.05–50.0
Ginga	LAC	pointed	CAT	1987-1991	1.5–30
ROSAT	PSPC, HRI	survey, pointed	CAT, UL	1990-1998	0.1–2.4
ASCA	GIS, SIS	pointed	CAT	1993-2000	0.4–12
INTEGRAL	ISGRI	pointed	UL	2000-2021+	20–100
<i>XMM-Newton</i>	EPIC-pn	slew, pointed	CAT, UL	2000-2021+	0.2–12
Swift	XRT	pointed	UL	2005-2021+	0.2–10.0

<sup>a</sup> Missions operate in survey, slew and/or pointed observation mode.

<sup>b</sup> Data source can be CATalogue and/or calculated Upper Limit (UL).

<sup>c</sup> Full energy range of the instrumentation.

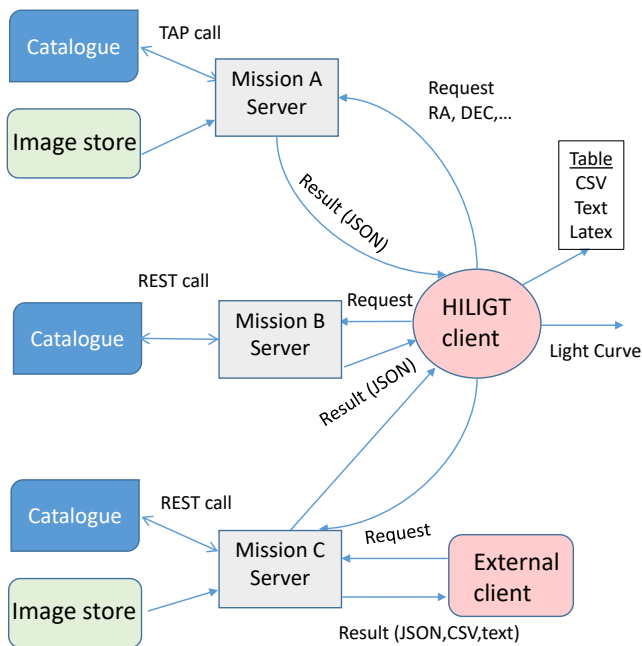


Figure 1: Information flow between servers and clients.

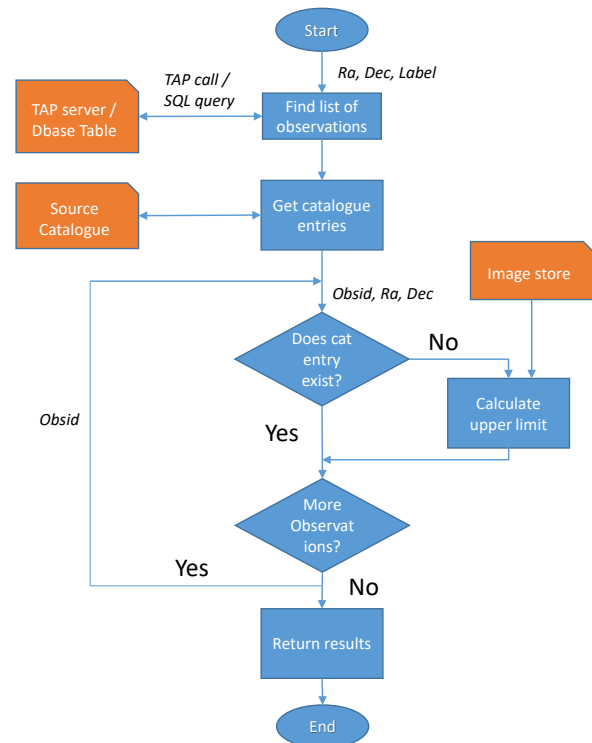


Figure 2: Flowchart of the design of a mission flux / upper limit server.

As technology has improved, there has been a tendency for the sensitivity of missions to increase and the beam size to decrease. This leads to quite different levels of output between the missions, e.g. *Vela 5B* has data for 99 sources, while the *XMM-Newton* point source catalogue contains almost 900,000 sources. A summary of the sky coverage and number of catalogued sources is given in Paper II (Table 1).

## 2.2. Input / output parameters

A definition of the input parameters accepted by the server is given in Table 2. As a minimum, a server needs to receive the coordinates of a sky position. A default spectral model of a power-law of spectral slope,  $\Gamma = 2$ , absorbed by a column of neutral hydrogen of  $3 \times 10^{20} \text{ cm}^{-2}$  is used for flux conversion and two-sigma upper limits are returned by default.

Note that for a meaningful comparison of flux between different missions it is essential that the spectral model used for the flux conversion is an accurate representation of the spectrum of the source in question. The *wrong* spectral model can artificially introduce strong apparent variability between missions (e.g. Page, 2015).

The server can be made to ignore catalogue values and recalculate results by setting the parameter *usecat=NO*.

Each mission server returns a Javascript Object Notation (JSON) structure containing the full set of fields described in Table 3, or comma-separated values (CSV) or text records containing a reduced, easy to display, output structure. The output fields contain the count rate, number of source counts, number of background counts, exposure time, flux calculated using the supplied model and ancillary information.

Count rates returned by the instrumentation, which as can be seen from Table 1 may be recorded over differing energy ranges (e.g. 0.3–2 keV and 2–10 keV for the Swift-XRT telescope) are converted into fluxes in the standard bands. Upper limits are available for all missions which have produced a database of images that can be analysed. Upper limits have been pre-calculated for the INTEGRAL Soft Gamma-ray Imager (IS-GRI) and stored in a database table (see Paper II).

## 2.3. Clients

Servers may be hosted anywhere, although they are currently all located at the European Space Astronomy Centre (ESAC)<sup>6</sup> and for convenience have been made accessible via a single REST call:

[http://xmmuls.esac.esa.int/ULService\\_passthru?MISSION=<mission>&ra=<ra>&dec=<dec>](http://xmmuls.esac.esa.int/ULService_passthru?MISSION=<mission>&ra=<ra>&dec=<dec>)

See Table 2 for the full set of input parameters. Any server compliant with the input and output parameters detailed in Tables 2 and 3 could be added.

An example terminal client written in Python is available for download from:

<http://xmmuls.esac.esa.int/hilight/scripts/hilight.py>

In addition an interactive, web-based client written in Javascript is available at:

<http://xmmuls.esac.esa.int/hilight>

The entry page of the web client (Fig. 3) allows sky positions to be entered as a coordinate pair, a target name, to be resolved by SIMBAD, or a text file containing a list of coordinates. The missions to be interrogated can be selected from the upper panel (Fig. 3). Standard energy bands, the spectral model for conversion of count rate to flux, the confidence level of the upper limit and whether to use catalogue values, may all be selected.

The web client returns a basic output page of results for each source position and mission, listing the observation date, count rate and fluxes for each observation and selected energy-band (Fig. 4). By clicking on "Advanced Settings" further fields may be selected for display from a top panel. From the output page the results may be saved into a text file, a csv file or downloaded into a L<sup>A</sup>T<sub>E</sub>X table ready to be inserted into a paper. A basic light curve plotting function, based on the ZingChart v2.8.6 tool<sup>7</sup>, may be invoked from the output page. Alternatively, a Python code to plot the results with greater flexibility may be used.<sup>8</sup>

## 3. Scientific Uses

HILIGT lends itself to long timescale variability analysis, to the search for transients and to broad-band spectral variability analysis. We briefly describe an example of each below.

### 3.1. Analysis of long-term light curves

The first quasar to be identified was 3C 273 in 1963 (Schmidt, 1963). This was first observed in X-rays by the satellite *Uhuru* in 1970 and has subsequently been a scientific or calibration target of all the major X-ray observatories, resulting in a rich dataset which covers its activity over the last 50 years. In Fig. 5 we show the time series of the 2–12 keV flux from 3C 273 observed between 1970 and 2020, extending the work of Soldi et al. (2008) who concentrated on observations taken between 1985 and 2006. The light curve is quite stable, having maintained a mean 2–12 keV flux of  $1.0 \times 10^{-10} \text{ erg s}^{-1} \text{ cm}^{-2}$  over the 50 year span (45 years in the source restframe;  $z=0.158$ ) with a peak-to-peak variation of a factor 4. We note that the minimum flux of  $5.5 \times 10^{-11} \text{ erg s}^{-1} \text{ cm}^{-2}$  was recorded on 2019-07-02 being  $\sim 20\%$  fainter than the previous minimum registered in July 2015 (Kalita et al., 2017). This long time series gives confidence that fluxes from old and new missions can sensibly be compared despite the widely differing beam sizes of the instrumentation.

### 3.2. Transient search

To know whether a new X-ray source is an interesting transient it is necessary to compare the measured flux with previous detections or upper limits. It is straightforward to write a script

<sup>6</sup>Note that the Swift-XRT server forwards the request onto a further server hosted within the Leicester Database & Archive Service (LEDAS) which actually makes the calculation.

<sup>7</sup><http://www.zingchart.com>

<sup>8</sup><http://xmmuls.esac.esa.int/hilight/scripts/lightcurve.py>

## High-energy Light-curve GeneraTor

### MISSION

XMM-New Slew  
Einstein

XMM-New Point  
Ginga

XMM-New Stacked  
Ariel-V

ROSAT Pnt  
ASCA

ROSAT Survey  
Heao1

INTEGRAL  
Vela5B

Swift-XRT  
Uhuru

EXOSAT

### TARGET NAME

### COORDINATES

### UPLOAD FILE

?

SUBMIT

### PARAMETERS

keV Range

XMM-Newton	0.2 - 2	2 - 12	0.2 - 12
Swift-XRT	0.2 - 2	2 - 12	0.2 - 12
ROSAT	0.2 - 2		

Upper limit significance

1 $\sigma$ 
2 $\sigma$ 
3 $\sigma$

Spectral model for flux conversion

Power law
Black body
?

NH [cm<sup>-2</sup>]

1x10<sup>20</sup>
3x10<sup>20</sup>
1x10<sup>21</sup>

Use catalogue values?

Yes
No

Figure 3: Input page for the HILIGT web client. Clicking on a mission selects it for processing, turning it from grey to bold white.





Figure 4: Output page for the HILIGT web client.

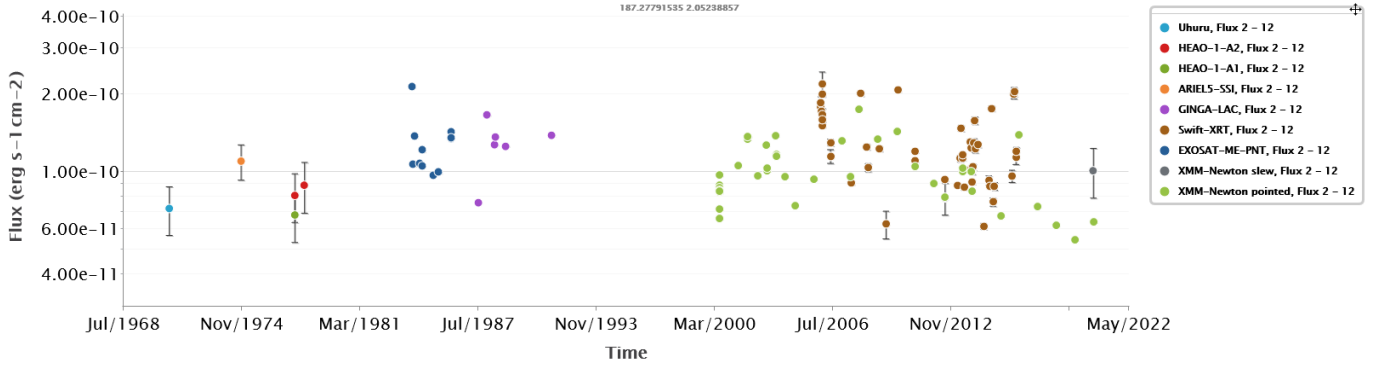


Figure 5: Light curve of the 2–12 keV flux from the QSO 3C 273 using the *Uhuru*, *Heao-1*, *Ariel-V*, *EXOSAT-ME*, *Ginga*, *Swift* and *XMM-Newton* flux servers. Flux conversion has been performed with a model of an absorbed power-law of slope 1.7 and galactic column of  $N_H = 1 \times 10^{20} \text{ cm}^{-2}$ . The plot has been produced by the ZingChart graphics tool integrated into HILIGT.

to extract and compare historical measurements at a given sky position from a set of the HILIGT flux and upper limit servers. An example plot for the light curve of the galaxy NGC 3599 is shown in Fig. 6. This candidate tidal disruption event (TDE) (Esquej et al., 2008; Saxton et al., 2015) exhibited an increase in flux of greater than a factor 100 between a *ROSAT* observation of 1993 and an *XMM-Newton* slew observation made in 2002, before decaying back to a quiescent state.

### 3.3. Search for spectral variability

By plotting the soft and hard energy band long-term light curves a simple check for spectral variability can be achieved. In Fig. 7 we show the light curve of the Seyfert I galaxy, NGC 985 in the 0.2–2 and 2–12 keV bands. It can be seen that the source spectrum hardened considerably in 2013, due to the soft flux diminishing while the hard flux remained stable at historical levels. This spectral change has been attributed to the development of a multi-component warm absorber around 2013 which preferentially absorbed the soft X-rays (Ebrero et al., 2016).

## 4. Access

While the extraction of count rates from catalogues is quite quick, the calculation of upper limits from images is a slower process. This limits the size of queries which can practically be issued to the system and, for the moment, the web client only accepts input files with up to ten sky positions. Larger queries may be built by using clients which poll the individual servers one source at a time.

A new strategy to increase the efficiency of the system by pre-calculating and storing *XMM-Newton* upper limits (RapidXMM; Ruiz et al., 2021) has been developed and will be integrated into HILIGT in the near future. This will greatly increase the throughput of the system and allow large queries to be processed for the *XMM-Newton* servers.

## 5. Conclusion and future plans

We have presented a system (HILIGT) for finding the flux recorded at a particular sky position for all X-ray observations. The system consists of a set of RESTful servers which may be called by any suitable client. A web-based client, capable of saving the historical flux in a number of formats and plotting the results has been introduced. The servers and client were made public on September 9th 2019.

The science available from HILIGT would benefit greatly from the addition of flux servers for current missions such as *Chandra*, *NuSTAR*, *NICER*, *MAXI* and *eROSITA* as well as extension to earlier missions such as *RXTE* and *BeppoSAX*.

The system for pre-calculating and storing *XMM-Newton* upper limits should be extended to other commonly used missions (*ROSAT*, *EXOSAT*, *Einstein*) to maximise the efficiency and usefulness of the system.

Finally, we note that HILIGT may prove useful for cross-calibration studies between X-ray missions.

## 6. Acknowledgments

We acknowledge support from ESA through the Faculty of the European Space Astronomy Centre (ESAC) - Funding reference 560/2019 and under the ESAC trainee program of 2018.

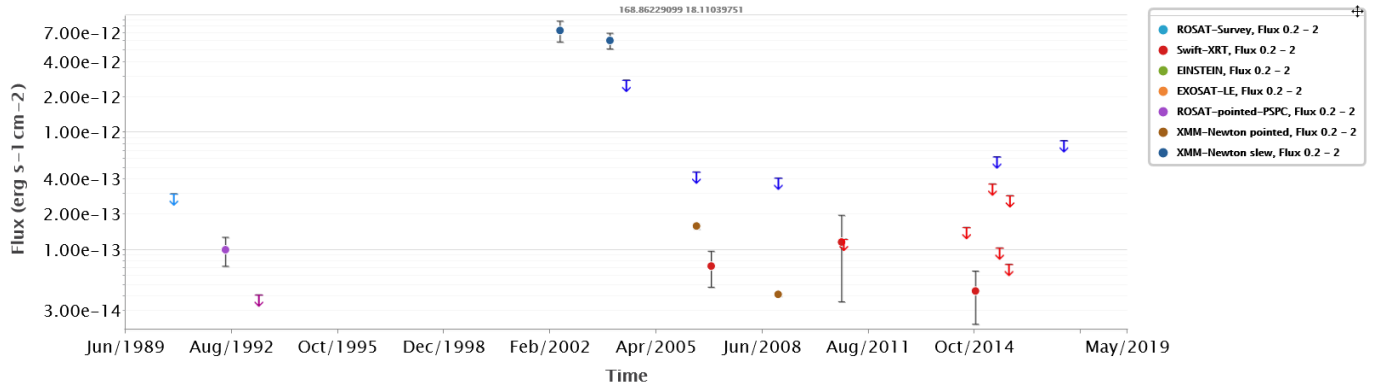


Figure 6: Full light curve of the 0.2–2 keV flux from the candidate tidal disruption event NGC 3599 using the *ROSAT*, *Swift* and *XMM-Newton* flux servers. Count rates have been converted into flux using a spectral model of a  $kT=60$  eV black-body absorbed by a galactic column of  $N_H = 1 \times 10^{20} \text{ cm}^{-2}$  (see [Esquej et al., 2008](#); [Saxton et al., 2015](#)).

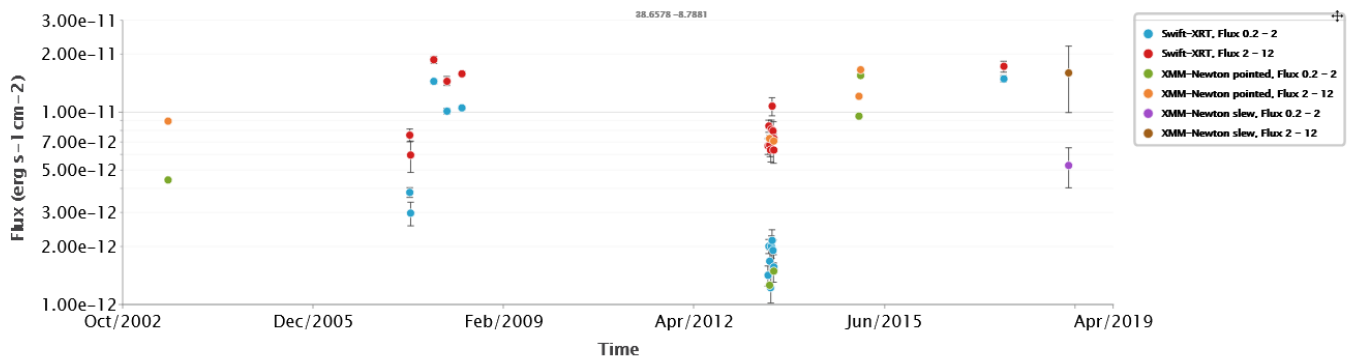


Figure 7: Light curve of the 0.2–2 keV (green, blue and purple points) and 2–12 keV (orange, red and brown points) flux from the AGN NGC 985 using the *XMM-Newton* and *Swift* flux servers.



## References

- Dowler, P., Rixon, G., Tody, D., Demleitner, M., 2019. Table Access Protocol Version 1.1. IVOA Recommendation 27 September 2019. URL: <https://ui.adsabs.harvard.edu/abs/2019ivoa.spec.0927D>.
- Ebrero, J., Kriss, G.A., Kaastra, J.S., Ely, J.C., 2016. Discovery of a fast, broad, transient outflow in NGC 985. *A&A* 586, A72. doi:10.1051/0004-6361/201527495, [arXiv:1511.07169](https://arxiv.org/abs/1511.07169).
- Esquej, P., Saxton, R.D., Komossa, S., Read, A.M., Freyberg, M.J., Hasinger, G., García-Hernández, D.A., Lu, H., Rodríguez Zaurín, J., Sánchez-Portal, M., Zhou, H., 2008. Evolution of tidal disruption candidates discovered by XMM-Newton. *A&A* 489, 543–554. doi:10.1051/0004-6361:200810110, [arXiv:0807.4452](https://arxiv.org/abs/0807.4452).
- Evans, I.N., Primini, F.A., Glotfelty, K.J., Anderson, C.S., Bonaventura, N.R., Chen, J.C., Davis, J.E., Doe, S.M., Evans, J.D., Fabbiano, G., Galle, E.C., Gibbs, Danny G., I., Grier, J.D., Hain, R.M., Hall, D.M., Harbo, P.N., He, X.H., Houck, J.C., Karovska, M., Kashyap, V.L., Lauer, J., McCollough, M.L., McDowell, J.C., Miller, J.B., Mitschang, A.W., Morgan, D.L., Mossman, A.E., Nichols, J.S., Nowak, M.A., Plummer, D.A., Refsdal, B.L., Rots, A.H., Siemiginowska, A., Sundheim, B.A., Tibbetts, M.S., Van Stone, D.W., Winkelman, S.L., Zografou, P., 2010. The Chandra Source Catalog. *ApJS* 189, 37–82. doi:10.1088/0067-0049/189/1/37, [arXiv:1005.4665](https://arxiv.org/abs/1005.4665).
- Evans, P.A., Page, K.L., Osborne, J.P., Beardmore, A.P., Willingale, R., Burrows, D.N., Kennea, J.A., Perri, M., Capalbi, M., Tagliaferri, G., Cenko, S.B., 2020. 2SXPS: An Improved and Expanded Swift X-Ray Telescope Point-source Catalog. *ApJS* 247, 54. doi:10.3847/1538-4365/ab7db9, [arXiv:1911.11710](https://arxiv.org/abs/1911.11710).
- Forman, W., Jones, C., Cominsky, L., Julien, P., Murray, S., Peters, G., Tananbaum, H., Giacconi, R., 1978. The fourth Uhuru catalog of X-ray sources. *ApJS* 38, 357–412. doi:10.1086/190561.
- Giacconi, R., Gursky, H., Paolini, F.R., Rossi, B.B., 1962. Evidence for x Rays From Sources Outside the Solar System. *Phys. Rev. Lett.* 9, 439–443. doi:10.1103/PhysRevLett.9.439.
- Heararc Team, 1995. The HEASARC facility. volume 203. p. 139. doi:10.1007/978-94-011-0397-8\_13.
- Kalita, N., Gupta, A.C., Wiita, P.J., Dewangan, G.C., Duorah, K., 2017. Origin of X-rays in the low state of the FSRQ 3C 273: evidence of inverse Compton emission. *MNRAS* 469, 3824–3839. doi:10.1093/mnras/stx1108, [arXiv:1705.02721](https://arxiv.org/abs/1705.02721).
- Kaluzienski, L.J., 1977. Studies of Transient X-Ray Sources with the Ariel 5 All-Sky Monitor. Ph.D. thesis. National Aeronautics and Space Administration. Goddard Space Flight Center, Greenbelt, MD.
- Kraft, R.P., Burrows, D.N., Nousek, J.A., 1991. Determination of Confidence Limits for Experiments with Low Numbers of Counts. *ApJ* 374, 344. doi:10.1086/170124.
- Madsen, K.K., Beardmore, A.P., Forster, K., Guainazzi, M., Marshall, H.L., Miller, E.D., Page, K.L., Stuhlinger, M., 2017a. IACHEC Cross-calibration of Chandra, NuSTAR, Swift, Suzaku, XMM-Newton with 3C 273 and PKS 2155-304. *AJ* 153, 2. doi:10.3847/1538-3881/153/1/2, [arXiv:1609.09032](https://arxiv.org/abs/1609.09032).
- Madsen, K.K., Forster, K., Grefenstette, B.W., Harrison, F.A., Stern, D., 2017b. Measurement of the Absolute Crab Flux with NuSTAR. *ApJ* 841, 56. doi:10.3847/1538-4357/aa6970, [arXiv:1703.10685](https://arxiv.org/abs/1703.10685).
- Mukai, K., 1993. PIMMS and Viewing: proposal preparation tools. *Legacy vol. 3*, p.21–31. URL: <https://ui.adsabs.harvard.edu/abs/1993Legac...3...21M>.
- Nugent, J.J., Jensen, K.A., Nousek, J.A., Garmire, G.P., Mason, K.O., Walter, F.M., Bowyer, C.S., Stern, R.A., Riegler, G.R., 1983. HEAO A-2 soft X-ray source catalog. *ApJS* 51, 1–28. doi:10.1086/190838.
- Page, M.J., 2015. X-ray photometry. *MNRAS* 452, L45–L48. doi:10.1093/mnras/1slv084, [arXiv:1506.07015](https://arxiv.org/abs/1506.07015).
- Ruiz, A., Georgakakis, A., Gerakakis, S., Saxton, R., Kretschmar, P., Akylas, A., Georgantopoulos, I., 2021. The RapidXMM Upper Limit Server: X-ray aperture photometry of the XMM-Newton archival observations. *arXiv e-prints*, [arXiv:2106.01687](https://arxiv.org/abs/2106.01687).
- Saxton, R.D., Motta, S.E., Komossa, S., Read, A.M., 2015. Was the soft X-ray flare in NGC 3599 due to an AGN disc instability or a delayed tidal disruption event? *MNRAS* 454, 2798–2803. doi:10.1093/mnras/stv2160, [arXiv:1509.05193](https://arxiv.org/abs/1509.05193).
- Schmidt, M., 1963. 3C 273 : A Star-Like Object with Large Red-Shift. *Nature* 197, 1040. doi:10.1038/1971040a0.
- Sembay, S., Guainazzi, M., Plucinsky, P., Nevalainen, J., 2010. Defining High-Energy Calibration Standards: IACHEC (International Astronomical Consortium for High-Energy Calibration), in: Comastri, A., Angelini, L., Cappi, M. (Eds.), *X-ray Astronomy 2009: Present Status, Multi-Wavelength Approach and Future Perspectives*, pp. 593–594. doi:10.1063/1.3475350.
- Soldi, S., Türler, M., Paltani, S., Aller, H.D., Aller, M.F., Burki, G., Chernyakova, M., Lahteenmaki, A., McHardy, I.M., Robson, E.I., Staubert, R., Tornikoski, M., Walter, R., Courvoisier, T.J.L., 2008. The multi-wavelength variability of 3C 273. *A&A* 486, 411–425. doi:10.1051/0004-6361:200809947, [arXiv:0805.3411](https://arxiv.org/abs/0805.3411).
- Turner, T.J., Pounds, K.A., 1989. The EXOSAT spectral survey of AGN. *MNRAS* 240, 833–880. doi:10.1093/mnras/240.4.833.
- Warwick, R.S., Marshall, N., Fraser, G.W., Watson, M.G., Lawrence, A., Page, C.G., Pounds, K.A., Ricketts, M.J., Sims, M.R., Smith, A., 1981. The Ariel V /3 A/ catalogue of X-ray sources. I - Sources at low galactic latitude /absolute value of B less than 10 deg/. *MNRAS* 197, 865–891. doi:10.1093/mnras/197.4.865.
- Webb, N.A., Coriat, M., Traulsen, I., Ballet, J., Motch, C., Carrera, F.J., Koliopanos, F., Authier, J., de la Calle, I., Ceballos, M.T., Colomo, E., Chuard, D., Freyberg, M., Garcia, T., Kolehmäinen, M., Lamer, G., Lin, D., Maggi, P., Michel, L., Page, C.G., Page, M.J., Perea-Calderon, J.V., Pineau, F.X., Rodriguez, P., Rosen, S.R., Santos Lleo, M., Saxton, R.D., Schwope, A., Tomás, L., Watson, M.G., Zakardjian, A., 2020. The XMM-Newton serendipitous survey. IX. The fourth XMM-Newton serendipitous source catalogue. *A&A* 641, A136. doi:10.1051/0004-6361/201937353, [arXiv:2007.02899](https://arxiv.org/abs/2007.02899).
- Wood, K.S., Meekins, J.F., Yentis, D.J., Smathers, H.W., McNutt, D.P., Bleach, R.D., Byram, E.T., Chupp, T.A., Friedman, H., Meidav, M., 1984. The HEAO A-1 X-ray source catalog. *ApJS* 56, 507–649. doi:10.1086/190992.

Table 2: Input parameters of a server query.

Field	Data type	Units	range or options	Default	Description
mission	string	-	-	-	Name of mission <sup>a</sup>
ra	double precision	degrees	0.0 - 360.0	-	Right ascension
dec	double precision	degrees	-90.0 - +90.0	-	Declination
label	string	-	-	-	Source name
band	string	-	soft,hard,total,all	all	Energy band(s)
model	string	-	plaw,tbody	plaw	spectral model
specparam	float	- / keV	options <sup>b</sup>	2.0 or 100eV	slope or temperature
nh	float	cm <sup>-2</sup>	1.0E20, 3.0E20, 1.0E21	3.0E20	Column density
ulsig	int	sigma	1,2,3	2	Upper limit significance
usecat	bool	-	"yes","no"	"yes"	Use catalogue value?
FORMAT	string	-	"text","text/html","csv","JSON"	"text"	Output format

<sup>a</sup> Supported missions are: XMMpnt, XMMslew, XMMStacked, RosatSurvey, RosatPointedPSPC, RosatPointedHRI, Integral, ExosatLE, ExosatME, Einstein, Ginga, Ariel5, Heao1, SwiftXRT, Asca, Uhuru, Vela5B.

<sup>b</sup> Currently supported values are: slope=0.5,1.0,1.5,1.7,2.0,2.5,3.0,3.5 or black-body temperature=0.06,0.1,0.3,1.0 keV.

Table 3: Output fields of a server record.

Field	Data type	Units	range or options	Description
start_date	string	-	-	Start of obs - e.g. 2004-11-19T04:34:09
end_date	string	-	-	End of obs - e.g. 2004-11-19T05:47:35
crate	float	counts / second	-	Count rate
crate_err	float	counts / second	-	Count rate error
crate_flux	float	erg s <sup>-1</sup> cm <sup>-2</sup>	-	Source flux
crate_flux_err	float	erg s <sup>-1</sup> cm <sup>-2</sup>	-	Error on source flux
ul	float	counts / second	-	Upper limit on count rate
ul_flux	float	counts / second	-	Upper limit of flux
ulsig	int	-	-	Sigma of upper limit
obsid	string	-	-	Observation identifier
src_counts	int	counts	-	Counts in source region
bck_counts	int	counts	-	Counts in bckgnd region
exptime	float	seconds	-	Exposure time
filt	string	-	-	Filter
image	string	-	-	Name of image
bkgimage	string	-	-	Name of background image
expmap	string	-	-	Name of exposure map
eef	float	-	-	Encircled energy fraction
elow	float	keV	-	Lowest energy of band
ehigh	float	keV	-	Highest energy of band
mission	string	-	-	Name of mission, e.g. XMM-Newton
instrum	string	-	-	Name of instrument, e.g. EPIC-pn
ra	double precision	degrees	0.0 - 360.0	Right ascension
dec	double precision	degrees	-90.0 - +90.0	Declination
label	string	-	-	Source name
model	structure <sup>a</sup>	-	-	spectral model
status	string	-	"OK","NoData"	status for this instrument

<sup>a</sup> This is a JSON structure containing: Column density (cm<sup>-2</sup>), spectral model ("plaw" or "tbody") and spectral parameter (power-law index or black-body temperature in keV).